

## NOTES AND CORRESPONDENCE

## Errors in Radio Acoustic Sounding of Temperature

WAYNE M. ANGEVINE

*Cooperative Institute for Research in Environmental Sciences, NOAA Aeronomy Laboratory, Boulder, Colorado*

W. L. ECKLUND

*NOAA Aeronomy Laboratory, Boulder, Colorado*

1 June 1993 and 21 October 1993

## ABSTRACT

With the use of simultaneous correction for radial wind, the accuracy of radio acoustic sounding systems for the measurement of temperature has been substantially improved. The temperature accuracy can now be affected by a number of factors that have been considered negligible in previous work. This paper describes two types of errors, those due to atmospheric effects and those due to approximations in the temperature retrieval equation. The errors are examined in a set of convective boundary layer RASS and radiosonde data. In the category of atmospheric effects, two errors are computed. The first is caused by a range error due to the gradient of signal strength. This range error is newly proposed and is approximately  $0.05^{\circ}$ – $0.1^{\circ}\text{C}$ . The second is an error due to wind and turbulence of about  $0.1^{\circ}\text{C}$ . Commonly used approximations for factors in the retrieval equation contribute errors of a few tenths of a degree Celsius. A significant difference remains after these two corrections have been applied to the sample data.

## 1. Introduction

Radio acoustic sounding systems (RASS) for the remote measurement of temperature are now deployed routinely in field experiments and at long-term sites as simple additions to wind profiling radars. Recent improvements in RASS techniques, especially the use of simultaneous correction for radial wind, have increased the accuracy of RASS to the point where previously negligible errors may be important. An error of 0.3 K at 300 K ( $27^{\circ}\text{C}$ ) is only a 0.1% error, so error terms as small as 0.01% (parts in  $10^4$ ) may be significant. This paper describes two categories of RASS errors, those due to atmospheric effects and those due to approximations in the temperature retrieval equation.

A RASS measures temperature with a Doppler radar and one or more acoustic sources (Matuura et al. 1986; May et al. 1988; May et al. 1990). The acoustic sources are located near the radar antenna, and the radar measures the speed at which the acoustic wave propagates. Recently, the Aeronomy Laboratory has devised several enhancements to RASS (Angevine et al. 1994). The most important of these is the ability to measure the acoustic velocity and the wind velocity simultaneously,

and thereby remove the largest source of error identified in previous studies of RASS accuracy (May et al. 1989).

The boundary-layer wind profiler was developed by the National Oceanic and Atmospheric Administration (NOAA) Aeronomy Laboratory and is described in Ecklund et al. (1988). It is a relatively compact and portable system operating at a frequency of 915 MHz. Table 1 shows the basic characteristics of the profiler/RASS. In the experiment described here, the profiler cycled through five different beam directions in sequence. The data presented here are from vertical beams only. Each beam position was sampled for 30 s and moving the antenna between positions took 10 s, so the vertical beam was sampled every 200 s. The vertical resolution (range gate length) was 100 m, and the minimum height was 147 m. The acoustic excitation was continuous at constant amplitude with frequencies chosen randomly from within a selected window (Angevine et al. 1994). A different frequency was selected every 25 ms.

The data reported here are from the Rural Oxidants in the Southern Environment II (ROSE II) Experiment in June 1992. The RASS was in a clearing in a pine plantation in west-central Alabama. The RASS was operated from a trailer that also contained the radio-sonde equipment, a National Center for Atmospheric Research (NCAR) Cross-chain Loran Atmospheric Sounding System (CLASS). Vaisala RS-80L radio-

---

*Corresponding author address:* Wayne M. Angevine, 325 Broadway R/E/AL3, Boulder, CO 80303.

TABLE 1. Boundary-layer profiler-RASS parameters.

Frequency	915 MHz
Peak power	500 W
Antenna	Microstrip array
Beamwidth	9°
Acoustic frequency	2000 Hz (nominal)
Acoustic power	30 W

sondes were used. During this period, the winds were generally light. The mean wind speed in the boundary layer during the periods surrounding each flight was approximately  $4 \text{ m s}^{-1}$ . The daytime convective boundary layer was 1100–1300 m deep and very turbulent. The mean temperature at midday at 150 m AGL was  $28^\circ\text{C}$ , the mean water vapor mixing ratio was  $12 \text{ g kg}^{-1}$ , and the mean virtual temperature was  $30.2^\circ\text{C}$ .

## 2. Results

Figure 1 shows the uncorrected mean difference and standard deviation of the difference of virtual temperature between the RASS and sonde for 31 flights on 13 days during ROSE II. The RASS measurement is an average over 30 min (8–10 individual samples) centered at the sonde launch time. All flights during these days are included except those in the early morning, when the radar reflectivity was low. The 31 flights included 9 in the midmorning (0900–1000 CST), 11 around 1200 CST, 7 in the midafternoon (1400–1500 CST), and 2 at night (1900–2000 CST). The pattern shown in Fig. 1 is present at all times. The difference is negative (the RASS indicates lower temperature than the sondes) at the lowest height, but quickly becomes positive (the RASS temperature is higher) as height increases, and then stays approximately constant above 400 m. The maximum difference is about  $0.8^\circ\text{C}$ . The standard deviation is about  $0.5^\circ\text{C}$ .

The sense of the errors in the following discussion and figures is that positive errors cause the virtual temperature calculated from the RASS to be higher than the actual virtual temperature.

## 3. Range error

The acoustic signal near 2 kHz used for RASS with the 915-MHz profiler is strongly attenuated in the atmosphere. This attenuation varies with temperature and humidity. In addition, the amount of acoustic energy in the radar beam, and therefore the returned signal, varies with height due to advection of the acoustic wave by the wind. These effects mean that the returned signal is not coming uniformly from all parts of the profiler range resolution cell.

The temperature measured by the RASS is a weighted average of the virtual temperature at each height. The weight is the relative signal strength from

that portion of the range resolution cell. The result is normalized by the total signal strength, so the measured temperature in cell  $m$  is

$$T_m = \frac{\int_{r-\delta r/2}^{r+\delta r/2} T(z)S(z)dz}{\int_{r-\delta r/2}^{r+\delta r/2} S(z)dz}, \quad (1)$$

where  $r$  is the range to the center of the cell,  $\delta r$  is the cell length,  $T$  is virtual temperature,  $S$  is signal strength, and  $z$  is range (height). This expression assumes that the radar range weighting function (Doviak and Zrnić 1993) is approximately the ideal “boxcar” shape. If we assume a linear temperature profile

$$T = T_0 + \gamma z, \quad (2)$$

where  $T_0$  is the virtual temperature at  $z = 0$  and  $\gamma$  is the virtual temperature lapse rate, the measured temperature in cell  $m$  is

$$T_m = T_0 + \gamma \frac{\int_{r-\delta r/2}^{r+\delta r/2} z 10^{az} dz}{\int_{r-\delta r/2}^{r+\delta r/2} 10^{az} dz}, \quad (3)$$

where  $a = a(z)$  is the signal strength at range  $z$  in decibels (dB). We assume a linear profile of signal strength in decibels and interpolate between the next lower and next higher gates, giving

$$a_m = - \frac{(Sdb_{m-1} - Sdb_{m+1})}{10(2\delta r)}, \quad (4)$$

where  $Sdb_p$  is the signal-to-noise ratio (SNR) measured by the RASS for the return from the acoustic signal

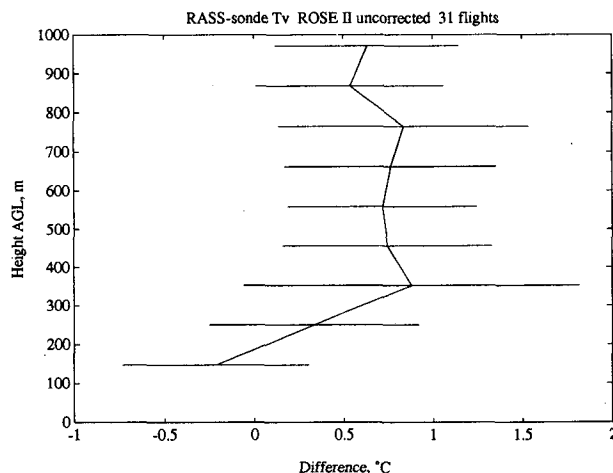


FIG. 1. Mean difference (RASS – sonde) of virtual temperature for 31 flights at ROSE II. RASS measurement is average over one-half hour centered on the sonde launch time. Horizontal bars are  $\pm 1\sigma$  of the average over the 31 periods.

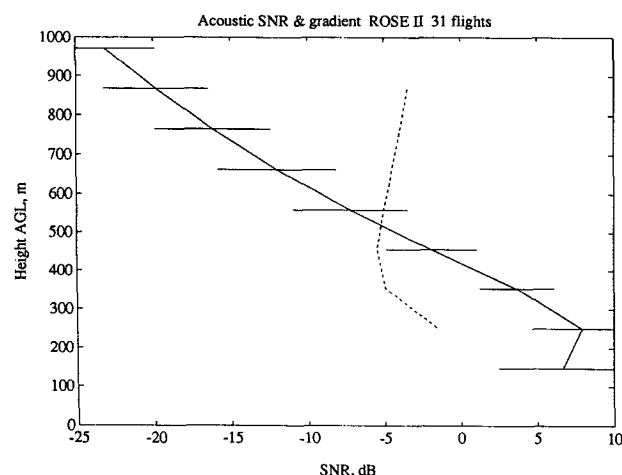


FIG. 2. Acoustic SNR (solid) and its gradient Eq. (4) [ $\text{dB} (100 \text{ m})^{-1}$ ] (dashed) for the 31 time periods. Horizontal bars are  $\pm 1\sigma$  of the SNR of the average over the 31 half-hour periods.

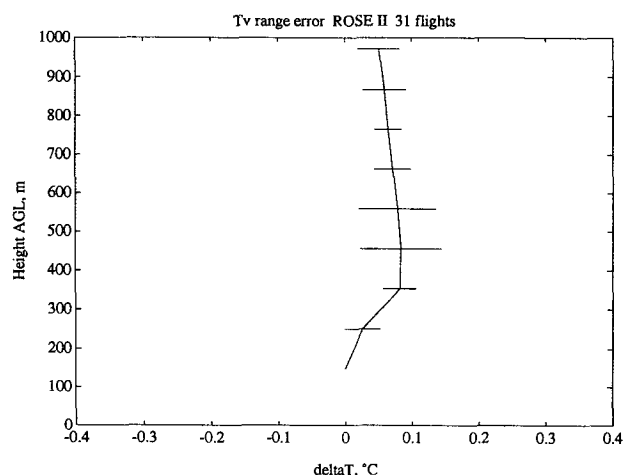


FIG. 4. Temperature error due to range error. Horizontal bars are  $\pm 1\sigma$  of the average over the 31 periods. Positive error means that calculated virtual temperature is higher than actual virtual temperature.

(the acoustic SNR) in range cell  $p$ . Here  $a_m$  is a constant for each range cell (a discrete rather than continuous function of  $z$ ). This is equivalent to taking the temperature at the centroid of the range cell, using the return signal strength as an analogy to mass. Therefore, we refer to the centroid as the "effective range." Since the origin of  $z$  is arbitrary, the temperature profile need not be linear over the entire height range, but only over the individual range gate.

The effective range was calculated for each of the 31 half-hour time periods corresponding to the sonde flights. Figure 2 shows the mean acoustic SNR and its gradient (4) for the 31-flight dataset. The standard deviation of the SNR is also shown for the 31 half-hour

periods. The gradient of SNR is near zero in the lowest range gates and approximately  $-5 \text{ dB} (100 \text{ m})^{-1}$  from 350 to 850 m AGL. This leads to a mean range error (difference of the effective range and the geometric range) of  $-5$  to  $-10$  m, as shown in Fig. 3. The resulting temperature error  $\Delta T_r$  is  $0.05^\circ$  to  $0.1^\circ\text{C}$ , shown in Fig. 4. The correction will vary with the range resolution (size of range cell) and will be least severe with the smallest range cells (best range resolution).

#### 4. Wind and turbulence error

In addition to the range error discussed above, errors in the measurement of virtual temperature by RASS can be caused by vertical and horizontal winds and by the displacement of the acoustic source from the radar antenna (Peters 1994). The vertical winds are accounted for by the simultaneous correction technique used here (Angevine et al. 1994). A current theory (Lataitis 1992), which proposes turbulence as an additional contributing factor, predicts an error for the observed conditions (light winds and strong turbulence) that we refer to as the "wind and turbulence error"  $\Delta T_w$  as shown in Fig. 5.

The profiles of the RASS-sonde virtual temperature difference taking into account the range error and the wind and turbulence error are shown in Fig. 6. Profiles are shown for no correction, range correction only, and both corrections. The corrections are still insufficient to account for all of the observed difference, but together account for about 15% of the discrepancy in the middle range of heights (350–850 m AGL).

#### 5. Approximations in temperature retrieval

The speed of sound in air is

$$v = \left( \frac{\gamma RT}{M} \right)^{1/2}, \quad (5)$$

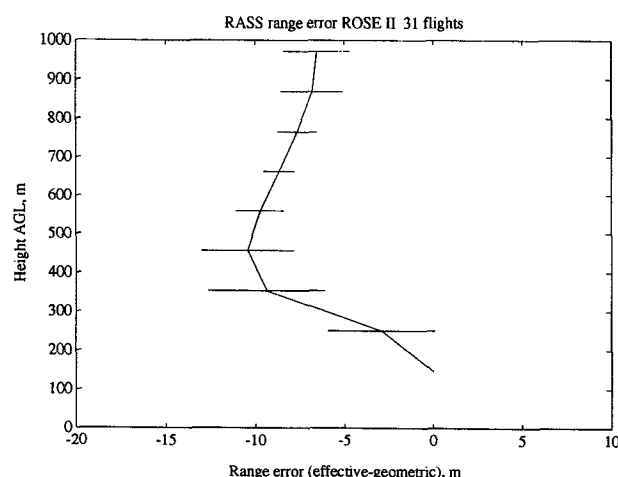


FIG. 3. Range error (difference of the effective range and the geometric range). Horizontal bars are  $\pm 1\sigma$  of the average over the 31 periods. Negative values indicate that effective range is less than geometric range.

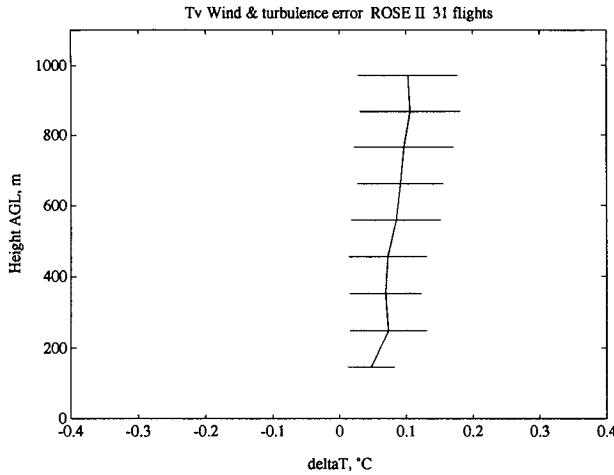


FIG. 5. Wind and turbulence error. Horizontal bars are  $\pm 1\sigma$  of the average over the 31 periods. Positive error means that calculated virtual temperature is higher than actual virtual temperature.

where  $\gamma$  is the ratio of specific heats,  $R$  is the universal gas constant,  $T$  is the kinetic temperature, and  $M$  is the molecular weight. Rearranging, the kinetic temperature is

$$T = \frac{v^2 M}{\gamma R}, \quad (6)$$

where  $\gamma$  and  $M$  are for the moist air and are not known. The molecular weight for dry air  $M_d = 28.964$  is used:

$$M_d = M \left[ \frac{1 + (q/\epsilon)}{1 + q} \right], \quad (7)$$

where  $q$  is the specific humidity and  $\epsilon = 0.622$  is the ratio of the molecular weight of water vapor to the molecular weight of air. The virtual temperature is

$$T_v = T \left[ \frac{1 + (q/\epsilon)}{1 + q} \right] = \frac{v^2 M_d}{\gamma R}, \quad (8)$$

so the change from  $M$  to  $M_d$  changes the measured quantity from kinetic to virtual temperature.

However, the virtual temperature the RASS system calculates is

$$T_{vc} = \frac{v_m^2 M'_d}{\gamma' R}, \quad (9)$$

where  $v_m$  is the measured sound speed,  $M'_d$  is the value of  $M_d$  used in the calculation, and  $\gamma'$  is the value of  $\gamma$  used in the calculation. The Aeronomy Laboratory data system uses  $M'_d = 28.96$  and  $\gamma' = 1.4$ . The sound speed is measured by

$$v_m = \frac{c_0 f_d}{2f}, \quad (10)$$

where  $c_0 = 2.998 \times 10^8 \text{ m s}^{-1}$  is the speed of light in a vacuum,  $f_d$  is the Doppler frequency, and  $f$  is the

radar carrier frequency. The resulting calculated virtual temperature is

$$T_{vc} = \frac{c_0^2 f_d^2 M'_d}{4 f^2 \gamma' R}. \quad (11)$$

The ratio of the actual virtual temperature to that calculated from the RASS measurement is

$$\frac{T_v}{T_{vc}} = \frac{c^2 \gamma' M_d}{c_0^2 \gamma M'_d}. \quad (12)$$

Since each of the errors is small, we will treat them individually in the presentation that follows.

The speed of propagation of radio waves in moist air differs from that in a vacuum according to

$$c = \frac{c_0}{n}, \quad (13)$$

where  $n$  is the refractive index of the medium (moist air). Bean and Dutton [1966, Eq. (1.17)] give an expression for  $n$ :

$$N = (n - 1) \times 10^6 \\ = 77.6 \frac{p}{T} + 3.73 \times 10^5 \frac{e}{T^2}, \quad (14)$$

where  $p$  is the total atmospheric pressure and  $e$  is the water vapor partial pressure, both in millibars. For example, if  $p = 1000 \text{ mb}$  and  $e = 42 \text{ mb}$  (saturated at  $30^\circ\text{C}$ ), not unreasonable conditions for the dataset used here,  $N = 426$  or  $n = 1.000426$ .

The ratio of specific heats  $\gamma$  is a complex function of atmospheric variables, most important among them being temperature and humidity. The determination of  $\gamma$  with sufficient accuracy for the purposes of this paper is still an active research topic. Cramer (1993)

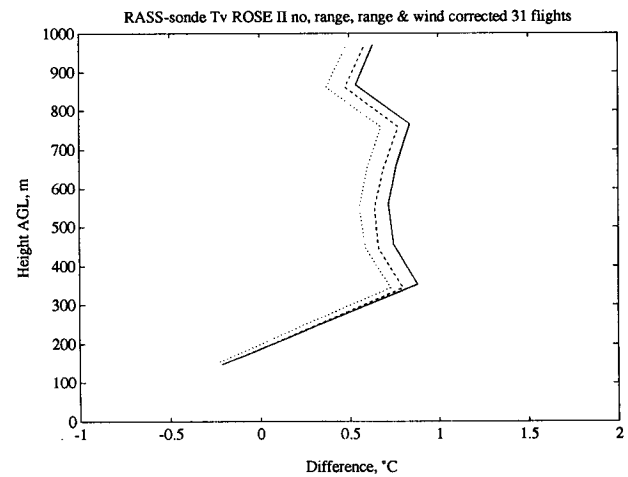


FIG. 6. Mean difference (RASS - sonde) of virtual temperature for 31 flights at ROSE II. Uncorrected (solid), range-corrected (dashed), and range-, wind-, and turbulence-corrected (dotted) differences are shown.

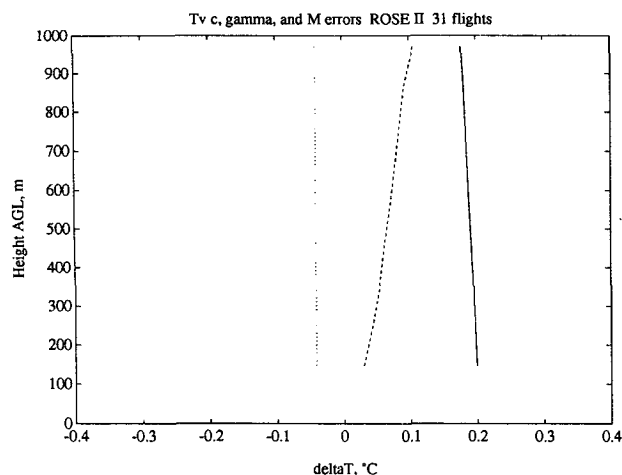


FIG. 7. Speed of light ( $c$  solid), ratio of specific heats ( $\gamma$ , dashed), and molecular weight ( $M$ , dotted) errors. Positive error means that calculated virtual temperature is higher than actual virtual temperature.

reviews the topic and gives an accurate formula. That formula when applied to the ROSE II dataset, assuming that the  $\text{CO}_2$  mole fraction is fixed at 314 ppm, yields values of  $\gamma$  between 1.3993 and 1.4015, with a mean value of 1.4003.

Figure 7 shows the speed of propagation, ratio of specific heats ( $\gamma$ ), and molecular weight errors as calculated from the ROSE II dataset. Figure 8 shows the sum of these errors with bars representing the standard deviation of the errors over the 31-flight average. The speed of propagation error is positive; that is, it causes the calculated temperature to be high. The  $\gamma$  error also causes the calculated temperature to be high. The molecular weight error is quite small. The corrections result in a significant total error of  $0.1^\circ\text{C}$ –

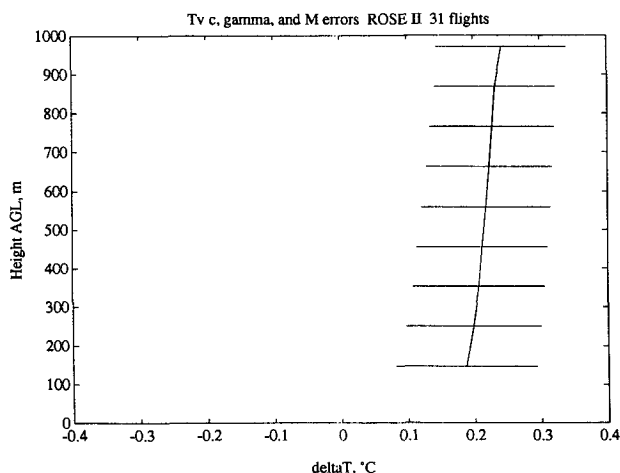


FIG. 8. Sum of  $c$ ,  $\gamma$ , and  $M$  errors. Horizontal bars are  $\pm 1\sigma$  of the average over the 31 periods.

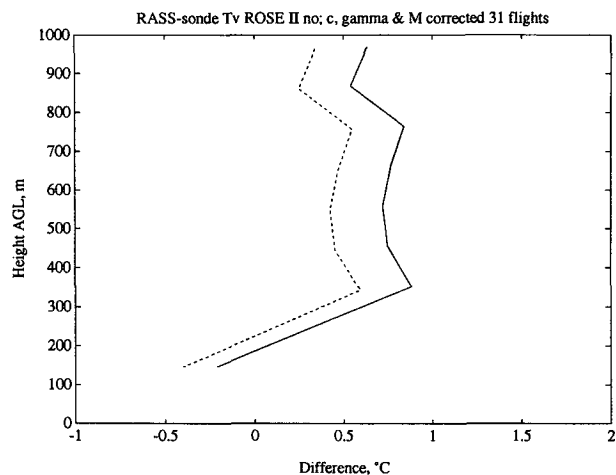


FIG. 9. Mean difference (RASS – sonde) of virtual temperature for 31 flights. Uncorrected (solid) and  $c$ ,  $\gamma$ , and  $M$  corrected (dashed).

$0.35^\circ\text{C}$  due to the approximations in the temperature retrieval equation. Figure 9 shows the difference between the RASS and sonde virtual temperatures with these errors corrected.

## 6. Conclusions

This study has considered new and recently proposed errors in RASS temperature measurements. Correcting for the new range error proposed here reduces the difference in virtual temperatures observed by the RASS and by radiosondes, as does correcting for the wind and turbulence error. Error terms previously assumed to be negligible in the temperature retrieval equation also significantly reduce the observed difference. Figure 10 shows the difference between the RASS and sonde

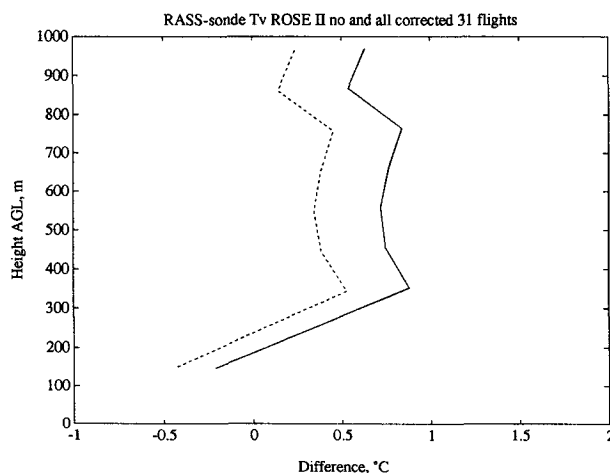


FIG. 10. Mean difference of virtual temperature for 31 flights. Uncorrected (solid) and corrected for range, wind, and turbulence,  $c$ ,  $\gamma$ , and  $M$ .

observations with all the corrections included. The total effect of all the corrections is a substantial reduction of the difference, from approximately  $0.7^{\circ}$  to  $0.3^{\circ}\text{C}$ .

RASS observations at other radar frequencies and in other atmospheric conditions would be subject to similar errors, but the relative importance of the various errors discussed here might well be different. For example, observations in the dry, cold, free troposphere would not have as large a speed of propagation error, but would have a larger  $\gamma$  error. Differences between RASS and sonde virtual temperature measurements similar to those shown here are reported by Moran and Strauch (1994) under rather different conditions using a 50-MHz RASS. Okrasinski and Olsen (1993) also observed a similar difference profile in a comparison between a 924-MHz RASS and sondes.

We considered whether errors in the radiosonde measurement might account for the difference that remains after the corrections are made. The difference is observed throughout the mixed layer where the profiles of temperature and humidity are smooth, so time lags in the sonde sensors should not be important. An error of approximately 25% in relative humidity ( $5^{\circ}\text{C}$  in dewpoint) would be required to cause a  $0.5^{\circ}\text{C}$  error in virtual temperature under these conditions. The specified accuracy of the CLASS system is 5% in relative humidity and  $0.5^{\circ}\text{C}$  in temperature.

We postulate that current theory is incomplete and that some effect or effects not yet understood cause the remaining observed difference. Even with this difference, the accuracy of the RASS measurements is comparable to that of existing radiosondes. It may be possible to use observations or refined theory to predict the shape of the systematic difference profile and remove it, thus further improving the RASS accuracy.

*Acknowledgments.* The ROSE II experiment was conducted in collaboration with the Southern Oxidant Study. The CLASS system was supplied by the NCAR

Surface and Sounding Systems Facility. Thanks to Richard Latatit of NOAA WPL for helpful discussions, to Jim Jordan of WPL for assistance with the equipment setup at ROSE II, and to Stuart McKeen and Michael Trainer of the Aeronomy Laboratory for launching some of the sondes. This research was supported in part by the Department of Energy under the Atmospheric Radiation Measurement Program.

#### REFERENCES

- Angevine, W. M., W. L. Ecklund, D. A. Carter, K. S. Gage, and K. P. Moran, 1994: Improved radio acoustic sounding techniques. *J. Atmos. Oceanic Technol.*, **11**, 42–49.
- Bean, B. R., and E. J. Dutton, 1966: *Radio Meteorology*. U.S. Dept. of Commerce, 435 pp.
- Cramer, O., 1993: The variation of the specific heat ratio and the speed of sound in air with temperature, pressure, humidity, and  $\text{CO}_2$  concentration. *J. Acoust. Soc. Am.*, **93**, 2510–2516.
- Doviak, R. J., and D. S. Zrnić, 1993: *Doppler Radar and Weather Observations*. Academic Press, 562 pp.
- Ecklund, W. L., D. A. Carter, and B. B. Balsley, 1988: A UHF wind profiler for the boundary layer: Brief description and initial results. *J. Atmos. Oceanic Technol.*, **5**, 432–441.
- Latatit, R. J., 1992: Theory and application of a radio-acoustic sounding system. NOAA Tech. Memo. ERL WPL-230, 207 pp.
- Matuura, N., Y. Masuda, H. Inuki, S. Kato, S. Fukao, T. Sato, and T. Tsuda, 1986: Radio acoustic measurement of temperature profile in the troposphere and stratosphere. *Nature*, **333**, 426–428.
- May, P. T., R. G. Strauch, and K. P. Moran, 1988: The altitude coverage of temperature measurements using RASS with wind profiler radars. *Geophys. Res. Lett.*, **15**, 1381–1384.
- , K. P. Moran, and R. G. Strauch, 1989: The accuracy of RASS temperature measurements. *J. Appl. Meteor.*, **28**, 1329–1335.
- , R. G. Strauch, K. P. Moran, and W. L. Ecklund, 1990: Temperature sounding by RASS with wind profiler radars: A preliminary study. *IEEE Trans. Geosci. Remote Sens.*, **28**, 19–28.
- Moran, K. P., and R. G. Strauch, 1994: The accuracy of RASS temperature measurements corrected for vertical air motion. *J. Atmos. Oceanic Technol.*, **11**, in press.
- Okrasinski, R. J., and R. O. Olsen, 1993: Intercomparison of remote and balloon-borne sensors. *Eighth Symp. on Meteorological Observations and Instrumentation*, Anaheim, CA, Amer. Meteor. Soc., 293–297.
- Peters, G., 1994: Measurements of momentum flux in the boundary layer by RASS. *J. Atmos. Oceanic Technol.*, **11**, 63–75.